AAIW05: ADCP/LADCP Cruise Report

Antarctic Intermediate Water Formation in the Southeast Pacific

21 August to 6 October 2005

Teresa K. Chereskin

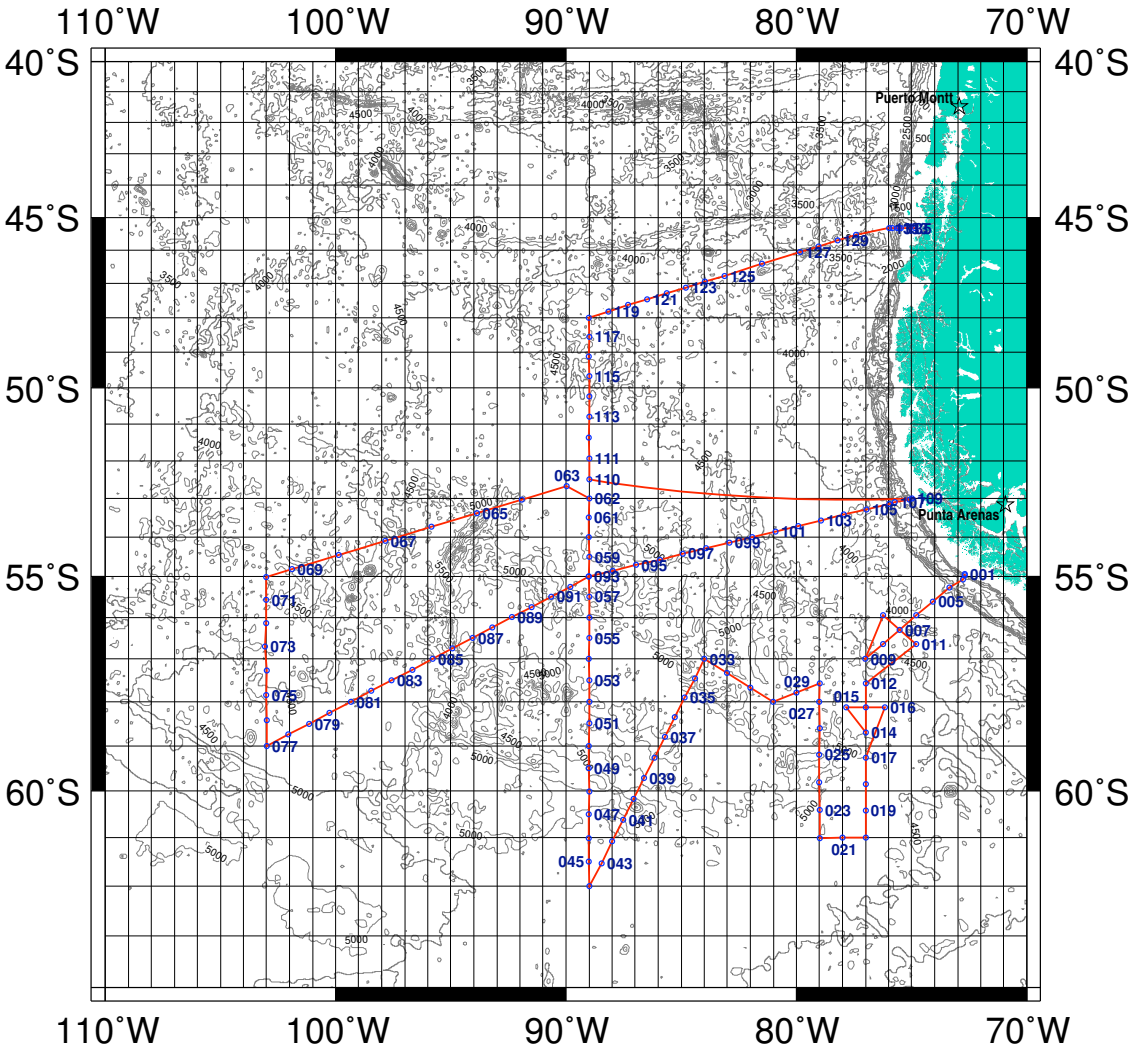

Figure 1: AAIW 2005 cruise track and station positions.

1 Introduction

A hydrographic survey consisting of LADCP/CTD/rosette stations, underway shipboard ADCP, XCTD profiling, float and drifter deployments in the southeast Pacific was carried out August to October 2005 (Fig. 1). The R/V Knorr departed Punta Arenas, Chile on 21 August 2005. A total of 135 LADCP/CTD/rosette stations were occupied, 399 XCTDs were launched, 13 ARGO floats and 20 surface drifters were deployed from 21 August - 6 October. Water samples (up to 24), LADCP and CTD data were collected, in most cases to within 10 meters of the bottom. Salinity, dissolved oxygen, and nutrient samples were analyzed from every bottle sampled on the rosette. Water samples were also measured for CO2 and CFCs, and underway surface pCO2, N2O, temperature, conductivity, oxygen, and meteorological measurements were made.

This report describes the acquisition and processing of the direct velocity measurements from hull-mounted shipboard acoustic Doppler current profilers (SADCPs) and from a Lowered Acoustic Doppler Current Profiler (LADCP) by the Chereskin lab group of Scripps Institution of Oceanography (SIO).

2 Shipboard ADCPs

2.1 Instrumentation

Data was recorded from two shipboard ADCPs: an Ocean Surveyor 75 kHz phased array (OS75) and an RD Instruments 150 kHz narrowband ADCP (NB150).

The OS75 is standard ship's equipment on R/V Knorr. The OS75 ADCP transducer was mounted in an instrument well located near the center line of the ship and below the laundry room. The well is open to the sea, and the transducer is located at approximately 5 m depth, with beam 3 oriented 45 deg to starboard.

The NB150 is an obsolete instrument, no longer supported by the manufacturer, that was installed by WHOI on request from the PI specifically for the AAIW cruise in order to profile currents at higher resolution and at shallower depths than the OS75. The NB150 ADCP transducer was mounted in an instrument well located below the lower lab at frame 85, about 8 feet starboard of the center line. The well is open to the sea, and the transducer is located at approximately 5 m depth, with beam 3 oriented 45 deg to starboard. The NB150 that was installed in Miami for AAIW failed prior to the ship's arrival in Punta Arenas, Chile. A second complete system was sent via air freight. Although the system had checked out satisfactorily at WHOI, it reported error messages after installation on Knorr. In actual use, the problem was very low signal on beam 2 (unsuitable for a 4-beam velocity solution); therefore we used a 3-beam solution.

2.2 Data acquisition

Single ping ADCP data from both instruments and ancillary navigation streams (GPS, gyrocompass, and POS/MV) were collected on a Dell 1-U rack-mounted server running the Linux operating system (Mandrake 10.2) using UHDAS, a data acquisition and processing software suite written by

Eric Firing and Jules Hummon, University of Hawaii.The data were processed in real-time on the Linux server (currents.knorr.whoi.edu) and were recorded in duplicate on a pair of internal, mirrored hard disks. Data were copied to Mac G4 laptops via a network (Samba) exported filesystem for further processing. The final datasets were processed post-cruise. The primary heading source was the ship's gyrocompass, and heading corrections were made using the POS/MV. The small number of POS/MV gaps were linearly interpolated (about 50 in all, scattered through the cruise). After applying the heading corrections, the overall additional calibration was an amplitude of 1.0 and a phase of 0.36 degrees for the NB150 and an amplitude of 1.0 and a phase of 0.174 for the OS75.

2.3 Sampling parameters

The NB150 operating parameters used during AAIW were 50 depth bins and an 8 m blank, range bin, and pulse length. The OS75 ADCP was configured to collect data in narrowband mode. The OS75 operating parameters were 70 depth bins and a 16 m blank, range bin, and pulse length.

2.4 Data processing

Overall, the quality of the navigation data acquired during AAIW was excellent. High precision GPS was available throughout the cruise, with an estimated single position fix accuracy of 1 m. The estimated accuracy of the POS/MV heading corrections is 0.1°(King and Cooper, 1992). The overall error in absolute currents is estimated at 1-2 cm s^{-1}(Chereskin and Harris, 1997). The main problems encountered were bubble sweepdown when the bow thruster was used to maintain station and during rough weather and heavy seas. The maximum profiling range of the OS75 was about 850 m, but this depth range was drastically curtailed when bubbles were severe.

The NB150 data were processed using a 3-beam solution. Where the data overlap with the OS75, they are of higher resolution. Unlike the OS75, he NB150 was not affected by bubbles from the bow thruster. It was negatively affected by bubble sweepdown during rough weather and heavy seas. The maximum range was about 225 m; typical range was 180 m.

The 2 ADCPs compared well over their common depth range. On-station comparison plots are available as a separate pdf document. The OS75 SADCP data were used as a constraint for the LDEO LADCP processing because of their greater range.

3 Lowered ADCP

3.1 Instrumentation

The lowered ADCP was Chereskin's 150 kHz RDI Phase 3 broadband ADCP, serial number 1394, firmware versions 1.16 (XDC), 5.52 (CPU), 3.22 (RCDR), and C5d3 (PWRTIM). The LADCP has custom 30° beam angles. It was mounted on the outer edge of the CTD rosette, about 1 inch above the bottom of the frame. A rechargeable lead acid gel cell battery in an oil-filled plastic case

(SeaBattery, Ocean Innovations, La Jolla, CA) was mounted in a steel box that was hose-clamped to the bottom of the rosette frame.

3.2 Data acquisition

A Mac G4 laptop computer running OSX (Panther 10.3.9) was used to upload an LADCP command set prior to each cast, using serial communication and a python terminal emulator (rditerm.py). Data acquired during the cast were stored internally on a 20 MB EPROM recorder. Data recovery used the terminal emulator, a public domain ymodem program (lrb), and a shell script to change the baud rate (change_baud) once the ymodem transfer was initiated. Eventually the shell script was made redundant when the terminal program was modified to change the baud rate for the data download.

3.3 Sampling protocol

Commands were uploaded from a file for deployment. The profiler was instructed to sample in a 2 ping burst every 2.6 seconds, with 0 s between pings and 1 s between (single-ping) ensembles, resulting in a staggered ping cycle of [1 s, 1.6 s]. Other relevant setup parameters were 16x16 m bins, 16 m blank, 16 m pulse, bandwidth parameter WB1, water mode 1, and an ambiguity velocity of 330 cm s^{-1}. Data were collected in beam coordinates.

The battery pack was recharged after every cast, using an AmRel linear programmable power supply. The power supply was set to 57.31 V constant voltage and 1.8 A maximum current. Typically, at the end of a cast, the power supply was current-limited at the maximum current. The power supply switched within about 10 min to constant voltage as the current level dropped. Charging was stopped nominally at 0.6 A in order to minimize the chance of overcharging, although the power supply resorts to trickle charging as the battery approaches full charge. Since lead acid gel cells outgas small amounts of hydrogen gas when overcharged/discharging, it is necessary to vent the pressure case. The pressure case was vented every few casts. There was a small but noticeable amount of outgassing.

3.4 Data processing methods

3.4.1 Background

The LADCP provides a full-depth profile of ocean current from a self-contained ADCP mounted on the CTD rosette. Using the conventional "shear method" for processing (e.g., Fischer and Visbeck, 1993), overlapping profiles of vertical shear of horizontal velocity are averaged and gridded, to form a full-depth shear profile. The shear profile is integrated vertically to obtain the baroclinic velocity and the resulting unknown integration constant is the depth-averaged or barotropic velocity. This barotropic component is then computed as the sum of the time-averaged, measured velocity and the ship drift (minus a small correction, less than 1 cm s^{-1}, to account for a nonconstant fall rate) (Fischer and Visbeck, 1993; Firing, 1998). Errors in the baroclinic profile accumulate as $1/\sqrt{(N)}$ where N is the number of samples (Firing and Gordon, 1990). This error translates to the lowest

baroclinic mode and, for a cast of 2500 m depth, it is about 2.4 cm s^{-1}(Beal and Bryden, 1999). The barotropic component is inherently more accurate, because the errors result from navigational inaccuracies alone. These are quite small with P-code GPS, about 1 cm s^{-1}(2 to 4 cm s^{-1}without). Comparisons with Pegasus suggest that the LADCP can measure the depth-averaged velocity to within 1 cm s^{-1}(Hacker et al., 1996). The rms difference between Pegasus and LADCP absolute profiles are within the expected oceanic variability, 3-5 cm s^{-1}(Send, 1994), due primarily to high frequency internal waves.

In previous experiments the previous ping interference (PPI), which results from the previous ping reflecting off the bottom and interfering with the current ping, affecting velocities in a small (100-m thick) layer about 750 m above bottom (for a sound speed of 1500 m s^{-1}), has caused a large data gap in the LADCP profile, causing an uncertain velocity offset (several cm s^{-1}) between the parts of the profile on either side of the gap. For this experiment bottom velocities were greatly improved by using Chereskin's instrument which pings asynchronously, thereby avoiding complete data loss in the interference layer. A second problem with data loss arises at the bottom of a CTD/LADCP cast, when the package is held 10 m above the sea bed for bottle sampling. At this distance the instrument is 'blind' since the blank after transmit is order 20 m, and a time gap in the data stream will result in an uncertainty in the absolute velocity. We attempted to minimize the stop at the bottom of the cast to keep this gap to a minimum.

3.4.2 UH CODAS

Initial processing was done with the University of Hawaii CODAS software. The method is the traditional shear method outlined in Fischer and Visbeck (1993) as implemented by Eric Firing in the UH CODAS LADCP software. The data were corrected for the local magnetic declination using geomag.m and the model output obtained from the NODC Geophysical Data Center. The rotated data were then loaded into a CODAS database. CTD time series data were available immediately following the cast and provided more accurate depth than from integrating LADCP vertical velocity as well as used to calculate sound speed at the transducer. Typically LADCP casts were analyzed through to absolute velocity, including CTD data, prior to the next station. The CODAS software includes a number of editing and quality control parameters. This report is not intended as a primer on the software, and parameter choices will not be discussed in detail, although many of them are discussed in Fischer and Visbeck (1993). The main ones used for the shear solution are set in the file merge.tmp (Table 1). The final data set is the one produced at sea.

Table 1: Explicit CODAS parameters set in merge.tmp after CTD data has been added for the second merge pass.

Parameter	value
w_bin0=	1
w_bin1=	5
u_bin0=	1
u_bin1=	5
u_pg_dif=	1
u_pg_min=	80
w_pg_dif=	1
w_pg_min=	80
w_ref_bin=	10
w_dif=	0.05
e_max=	0.1
min_correlation=	70
shear_dev_max=	3.5
shear_sum_dev_max=	1.5
clip_margin=	90
ping_secs=	0.0
min_wake_w=	0.1
wake_hd_dif=	20
wake_ang_min=	15
n_wake_bins=	2

3.4.3 LDEO version 8a

During the cruise, the casts were also processed with Martin Visbeck's LADCP Matlab processing routines, version 8a. The method (Visbeck, 2002) differs from the shear method in that an inverse technique is used which includes two additional constraints, the bottom velocity estimate and the average shipboard ADCP profile during the cast. In principle, the Firing shear and Visbeck inverse methods should agree when no additional constraints are included in the inverse, but at the moment the methods have shown unexplained differences on some data sets (Brian King, pers. comm.). The LADCP bottom velocity profile is calculated from the water track data when the bottom is in range. The v8a profiles were reprocessed after the cruise with two main changes: use the final edited shipboard ADCP and use the CODAS geomag routine in place of the LDEO magdev (substitution occurs in the local routine loadnav.m). The OS75 was the SADCP chosen to constrain the LADCP inverse because of its deeper range. The CODAS magnetic routines were substituted because time is a parameter in determining the magnetic declination, and it was observed that in some locations the value that geomag returned was about a degree different than the LDEO magdev value.

Table 2: Explicit LDEO parameters set in local mfiles.For v8a, these parameters were set in the wrapper run3_bb.m; for IX they were in set_cast_parameters.m.

Parameter	v8a	IX
p.pglim	0	0
p.elim	0.2	0.2
p.wlim	0.08	0.08
ps.down_up	0	0
ps.dz	20	20
p.avdz	ps.dz	20
p.weighbin1	1.0	1.0
p.btrk_mode	3	3
ps.botfac	1	1
ps.barofac	1	1
ps.shear	0	0
ps.sadcpfac	2	2
p.sadcp_dtok	.0035	0

3.4.4 LDEO version IX

Significant changes were made to the LDEO software, mainly in the weighting of the inverse solution, such that some of the parameters/behaviors of previous versions no longer exist. Use of the new release (IX) was a recommendation of the LADCP workshop held at the AGU Ocean Sciences 2006 meeting in Honolulu. As with v8a, the file loadnav.m was modified to use geomag.m from CODAS rather than magdev.m. Final OS75 shipboard ADCP data and bottom profiles calculated from watertrack data were used as constraints. Of the parameters that the 2 versions share, ps.sadcp_dtok was the only difference (Table 2). The v8a setting allows an extra 5 min (1 ensemble) of SADCP data on either side of the station to be included in the SADCP constraint.

3.5 Comparison of velocity solutions

Determining the bottom velocity profile from watertrack data is not as accurate as having bottom track data from the profiler. For this reason, the SADCP weight was set to 2 and the bottom profile weight to 1 for both LDEO versions. CODAS is unconstrained by these data. Differences were observed between all 3 sets of LADCP solution profiles as summarized in Table 3. A cast-by-cast comparison of the root-mean-square velocity differences for the solution pairs is given in Table 4 at the end of this document. The largest differences were between the CODAS and IX solutions, with an average root-mean-square difference (urms, vrms) over 135 profiles of (3.9, 4.4) cm s^{-1}. The smallest differences were between the CODAS and v8a solutions, with an average

root-mean-square difference (urms, vrms) of (2.6, 3.0) cm s^{-1}. The differences between the IX and v8a solutions were similar to the CODAS-v8a, with an average root-mean-square difference (urms, vrms) of (2.7, 3.2) cm s^{-1}.

Table 3: Mean rms differences over 135 stations.

	CODAS-IX cm s^{-1}	CODAS-v8a cm s^{-1}	IX-v8a cm s^{-1}
urms	3.9	2.6	2.7
vrms	4.4	3.0	3.2

Some example profiles are included to show the vertical structure of the differences. Generally, the agreement is good above 1000 m with larger differences below. There is a preferred ordering of the solutions, with the v8a velocity profile typically intermediate between the CODAS and IX solutions (e.g., Fig. 2). The v8a profile is usually closer to the CODAS one than to the IX one, both in the mean and in the shear profile, as quantified by the absolute mean and rms differences (Table 4). The bottom profile plotted is from the IX solution. If there are differences between IX and v8a in calculating the bottom profile, they are not noticeable in these plots since both profiles appear converge to the same bottom profile. Indeed, one of the most striking differences between IX and v8a is how different they can be through the water column while matching the same surface and bottom constraints. Fig. 3 is a profile from a station made just south of the Subantarctic Front. It is an example where the zonal velocity solution from v8a deviates by about 5 cm s^{-1} from the IX solution in the depth range 2000 m to 4000 m, then converges to the same bottom profile. Above 4500 m, the v8a and the CODAS zonal solutions agree fairly closely (within the v8a uncertainties). CODAS and v8a both estimate a deep zonal velocity averaged below 2000 m that is close to zero whereas the IX solution predicts westward flow. The IX shears disagree with the other solutions over this depth range. Meanwhile, the meridional velocity component shows much better agreement among all 3 solutions. Fig. 4 is an example where the zonal velocity solution compares well but the meridional one differs. This comparison is one of the highest vrms differences between CODAS and IX. A pdf document of the figures comparing solutions for each station is available separately.

Potential reasons for differences between the LDEO and CODAS solutions are differences in how the codes handle previous ping interference (PPI), smoothing and weighting of the inverse and the inclusion of surface/bottom constraints. The CODAS editing removes PPI. LDEO v8a ignores PPI; vIX can handle PPI either with its spike filter or with a dedicated PPI filter. The default for vIX was to use a spike filter but turn off the PPI filter; a comment in the code stated that the spike filter was more robust than the PPI filter in removing PPI when staggered pinging is used. The surface and bottom constraints should improve the LDEO solutions relative to the CODAS one, but it is difficult to judge the accuracy of the bottom velocity calculated from water track data. The inverse method provides error estimates, and both LDEO versions indicate reasonable uncertainties in their

respective solutions, with larger errors at greater depths. When the LDEO solutions disagree, the error bars are larger, but they often do not overlap (Figs. 3 and 4). This suggests that the differences between the LDEO solutions are due to changes in the code and not due to poor signal-to-noise ratio in the LADCP data. As noted, PPI and bottom tracking code changed between v8a and vIX. Additionally, the weighting of the inverse and the low-mode constraint changed between v8a and vIX. To further investigate the differences between these versions, the data for cast K104 were reprocessed using version IX but with the v8a method (ps.std_weight = 0) of weighting contraints. Changes in the solutions were subtle and did not account for the large observed differences (Fig. 5). A. Thurnherr (personal communication) suggested that if the weighting did not account for the changes, then it was most likely code related to explicit smoothing (ps.smoofac) and/or code related to removing large shears (ps.smallfac). A series of runs were done changing individual parameters. None of them resolved the cause of the differences between the LDEO solutions. Disabling the smallfac constraint (ps.smallfac=[1 0]) had a small effect (Fig. 6). Turning off the surface and bottom constraints made the IX solution look the most like 8a, except at the bottom of the profile (Fig. 7).

3.6 Comparison of depth-averaged velocity

The barotropic velocity is thought to be the most accurate LADCP velocity estimate. Fig. 8 compares the depth-averaged velocity for the 3 solutions. The agreement is reasonable, but there is a similar bias as observed in the profile data. IX barotropic velocity is the generally largest in magnitude, CODAS is smallest, and v8a is intermediate. An estimate of the barotropic tide from TPXO6.2, averaged over the duration of the cast, is shown for comparison. In some locations the tide can account for almost all of the barotropic current estimated by the LADCP (e.g., Firing, 1998), but that is not the case here. The tide appears somewhat correlated with the barotropic velocity, but much smaller in magnitude.

3.7 Conclusions

Because differences between the LDEO versions could not be resolved, the CODAS solutions will be used for final data. Although it would be preferable to include the SADCP as a formal constraint in the solution, the majority of CODAS LADCP profiles compare well with SADCP averaged over the corresponding time intervals.

Acknowledgements

Thanks are due to the SIO Oceanographic Data Facility for their outstanding support on the cruise, Eric Firing and Jules Hummon for UHDAS support and loan of the Dell used for SADCP acquisition, Lisa Beal for advice on LDEO v8a and Andreas Thurnherr for advice on LDEO vIX. Thanks also to Sharon Escher, Yueng-Djern Lenn and Yvonne Firing for their diligent watchstanding and processing efforts. Support was provided by the National Science Foundation Ocean Sciences Division Grant OCE-0327544.

References

Beal, L. M., and H. L. Bryden, The velocity and vorticity structure of the Agulhas Current at 32°S, *J. Geophys. Res., 104,* 5151-5176, 1999.

Chereskin, T. K., and C. L. Harris, Shipboard Acoustic Doppler Current Profiling during the WOCE Indian Ocean Expedition: I10, *Scripps Institution of Oceanography Reference Series, SIO-97-14,* 137 pp, 1997.

Firing, E. F. and R. Gordon, Deep ocean acoustic Doppler current profiling, *Proceedings of the IEEE Fourth International Working Conference on Current Measurements, Clinton, MD*, Current Measurement Technology Committee of the Ocean Engineering Society, 192-201, 1990.

Firing, E., Lowered ADCP development and use in WOCE, *It. WOCE Newsletter, 30,* 10-14, 1998.

Firing, E., Erratum, *Intl. WOCE Newsletter, 31,* 20, 1998.

Fischer, J. and M. Visbeck, Deep velocity profiling with self-contained ADCPs, *J. Atmos. and Oceanic Tech., 10*, 764-773, 1993.

Hacker, P., E. Firing, W. D. Wilson, and R. Molinari, Direct observations of the current structure east of the Bahamas, *Geophys. Res. Let., 23*, 1127-1130, 1996.

King, B. A. and E. B. Cooper, Comparison of ship's heading determined from an array of GPS antennas with heading from conventional gyrocompass measurements, *Deep-Sea Res., 40,* 2207-2216, 1993.

Send, U., The accuracy of current profile measurements - effect of tropical and mid-latitude internal waves, *J. Geophys. Res., 99,* 16229-16236, 1994.

Visbeck, M., Deep velocity profiling using lowered acoustic Doppler current profilers: bottom track and inverse solution, *J. Atmos. and Oceanic Tech., 19*, 795-807, 2002.

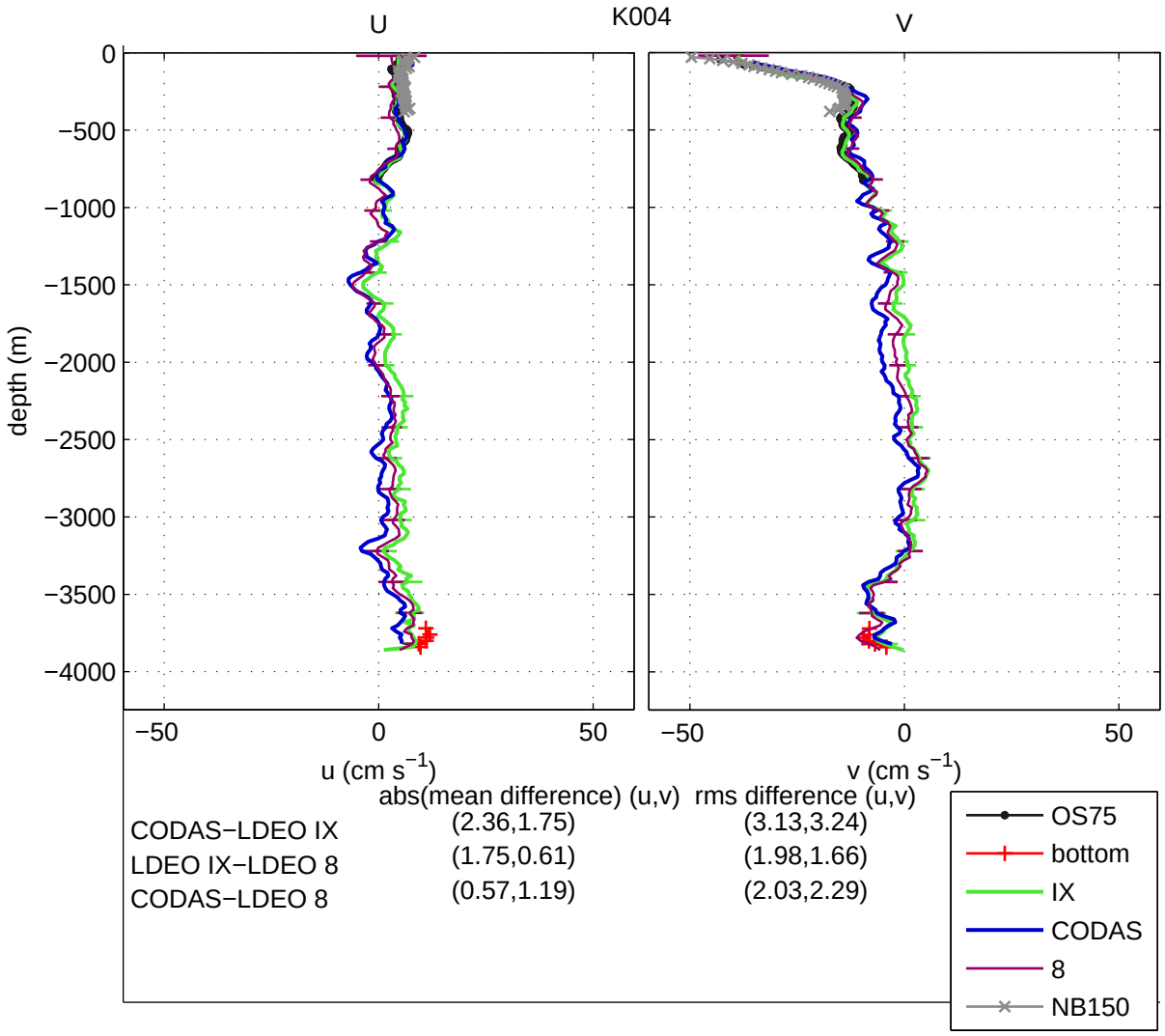

Figure 2: LADCP station 4

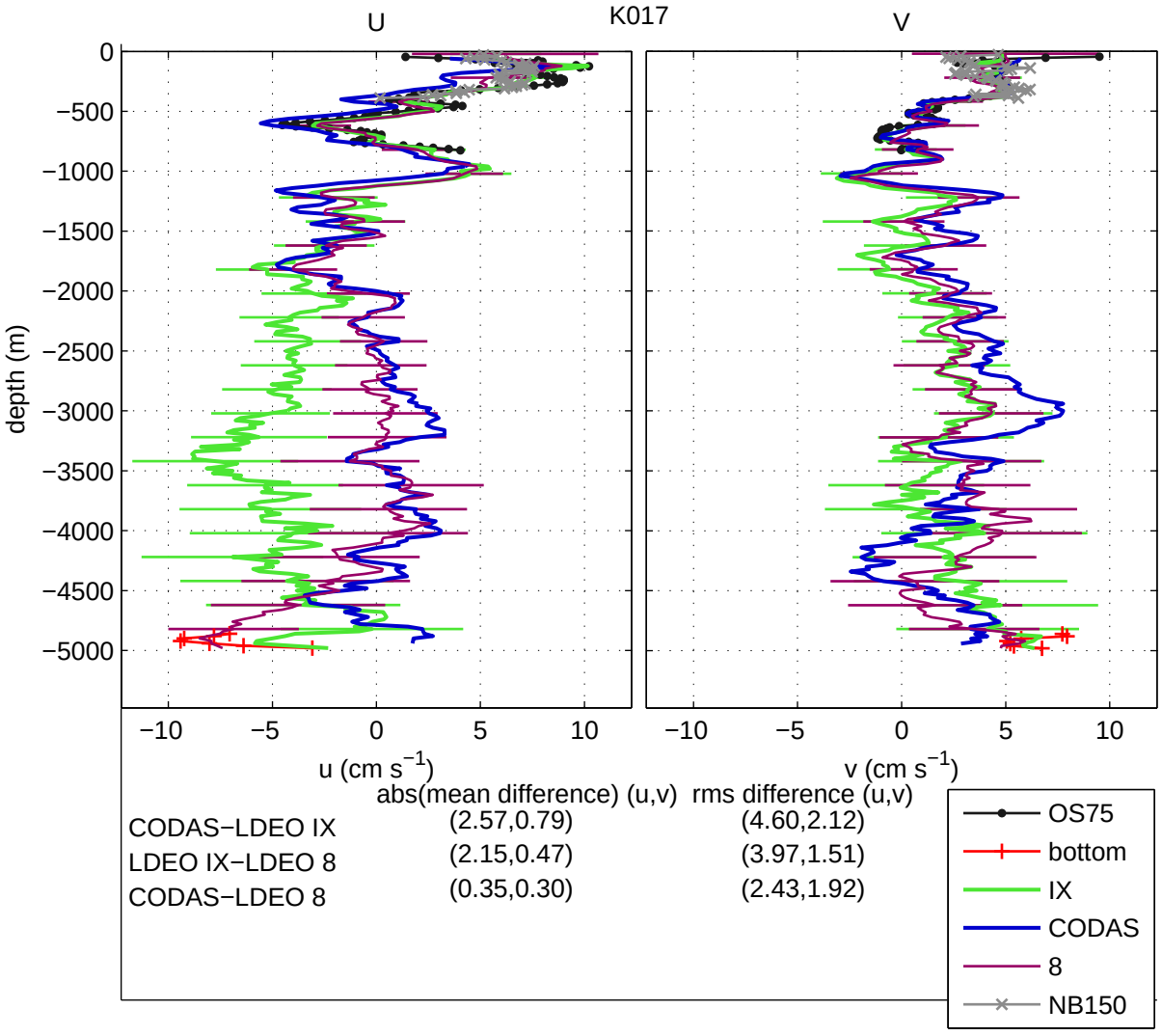

Figure 3: LADCP station 17

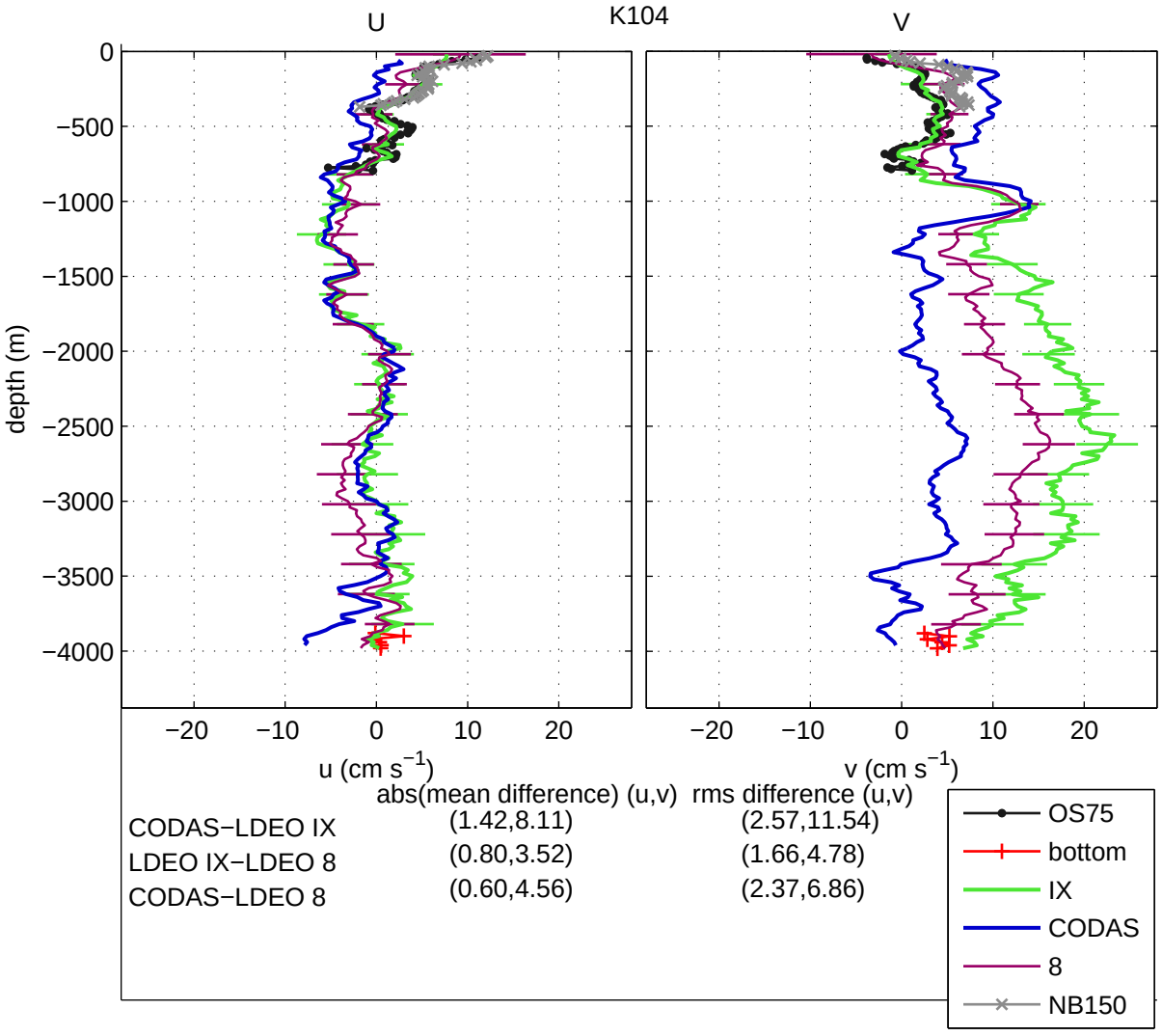

Figure 4: LADCP station 104

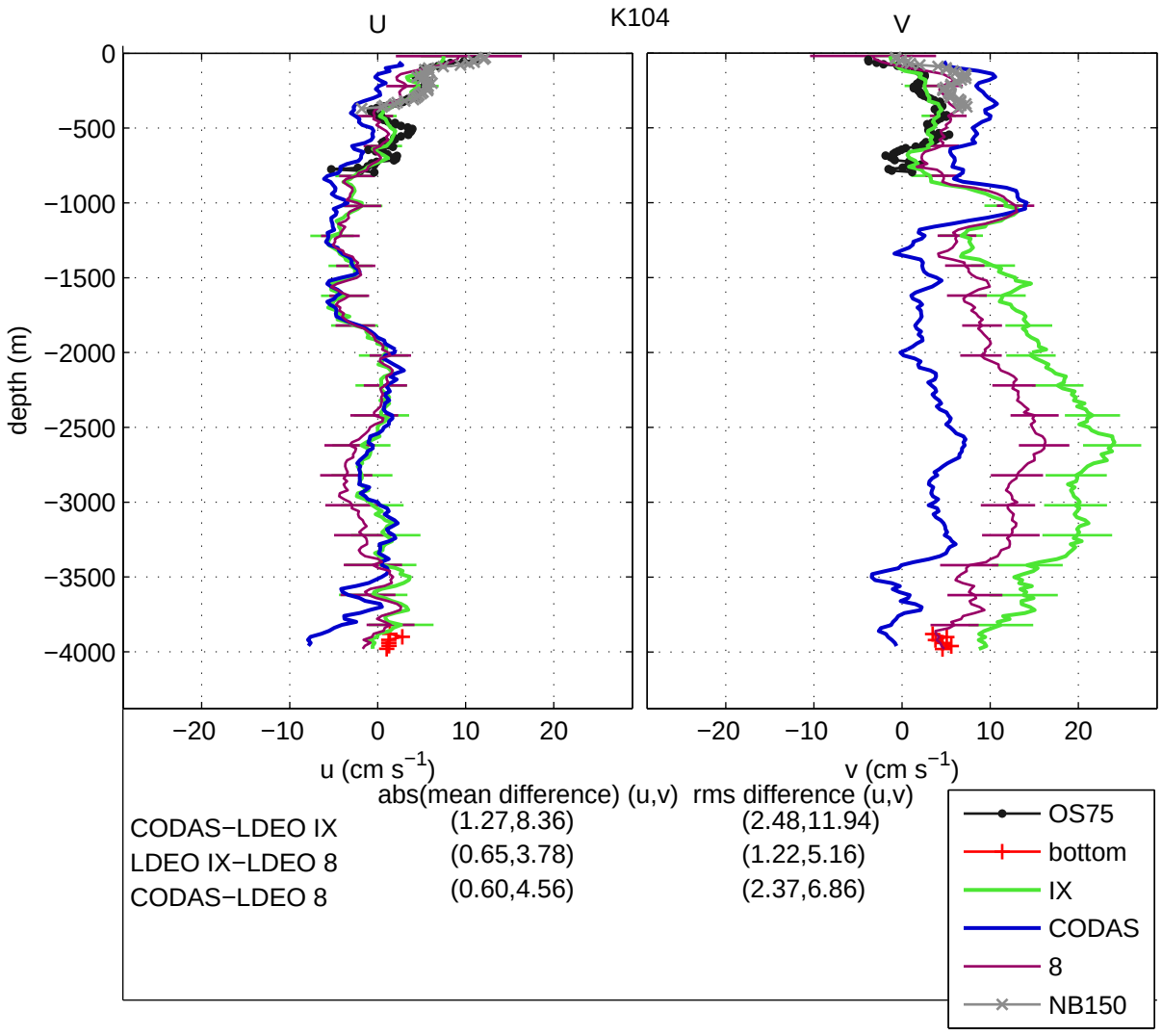

Figure 5: LADCP station 104. The IX version used the same weighting as v8a (ps.std_weight = 0).

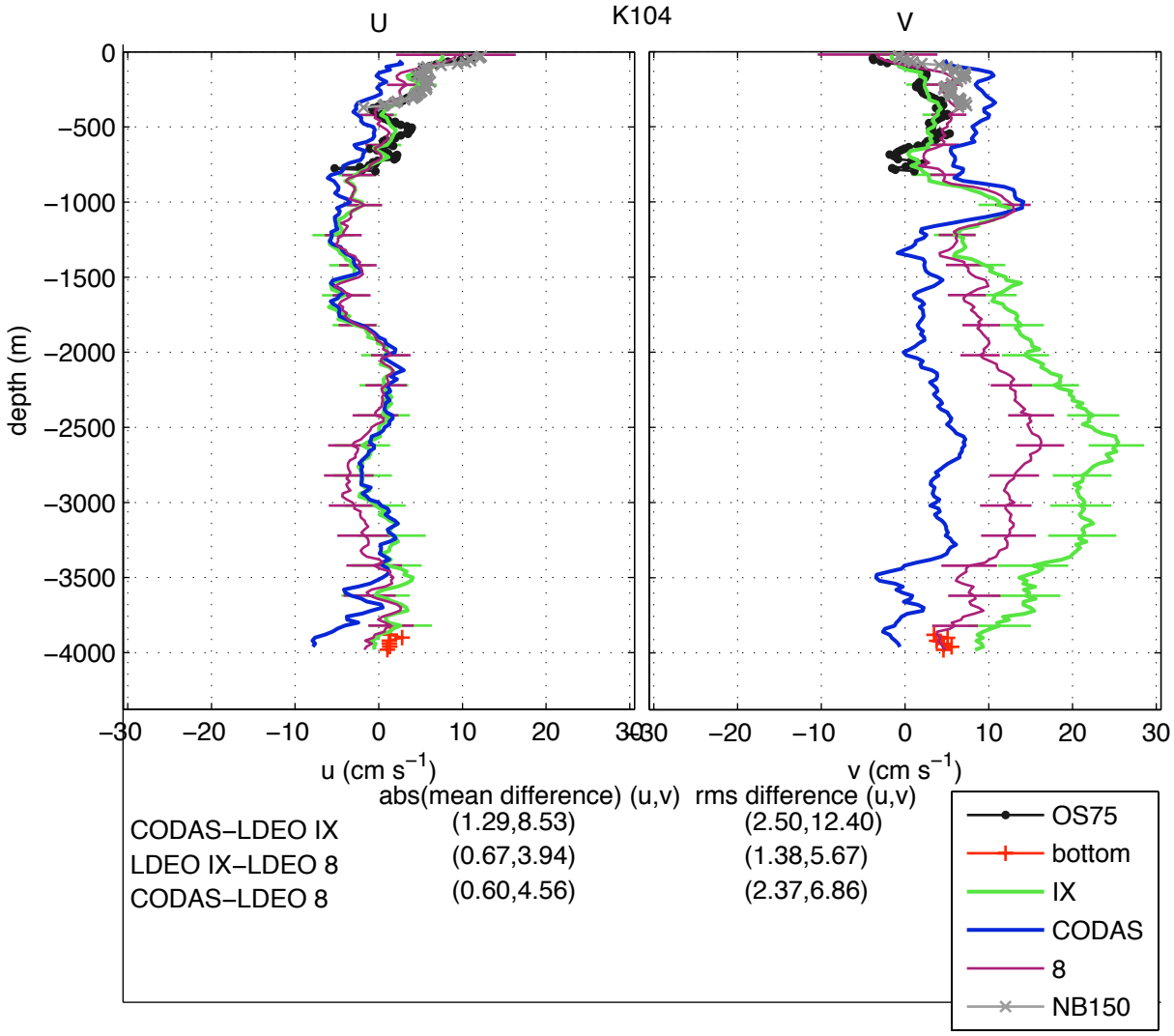

Figure 6: LADCP station 104. The IX version disabled the removal of large shears (ps.smallfac = [1 0]).

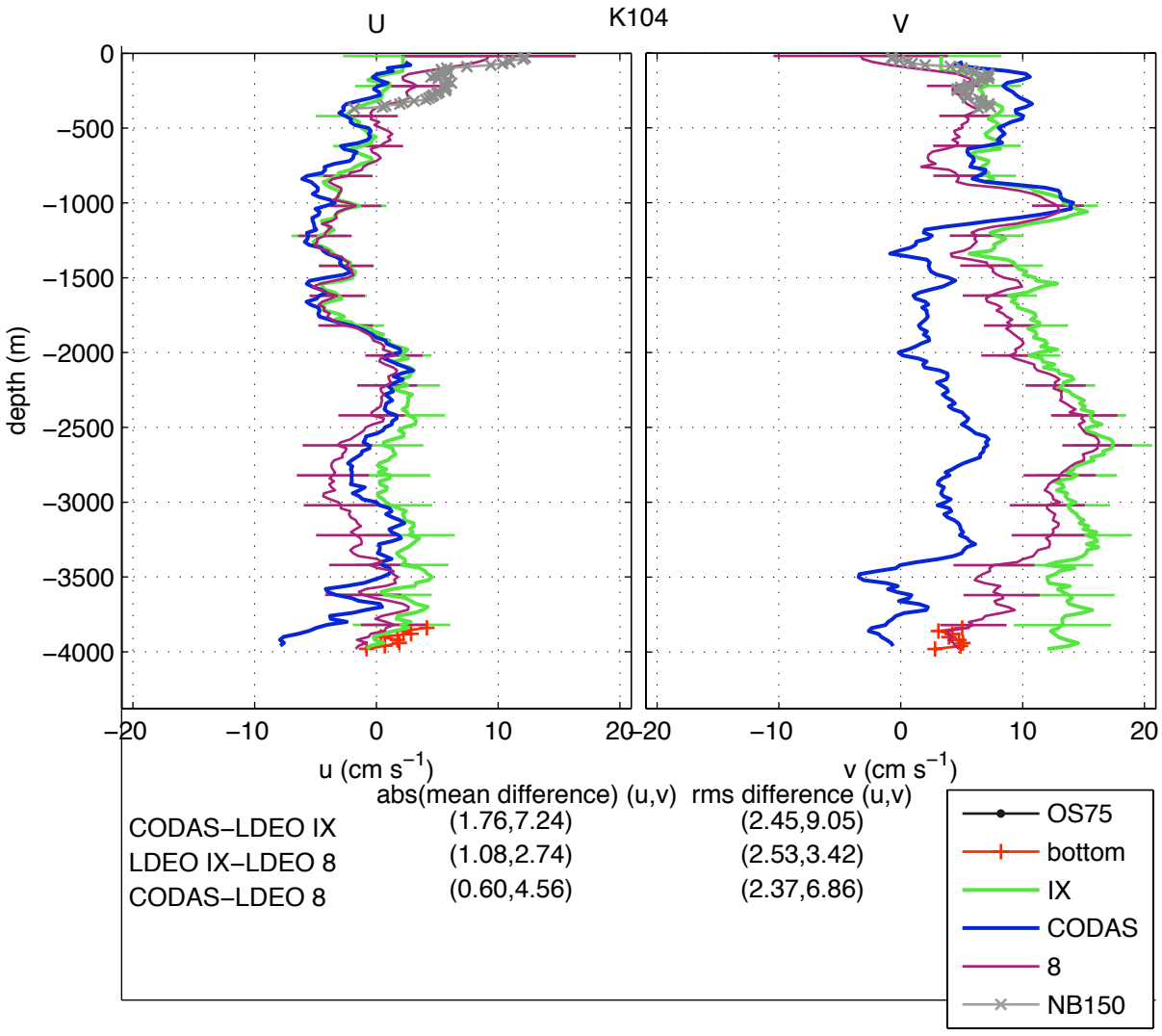

Figure 7: LADCP station 104. The IX version does not use any surface or bottom constraints.

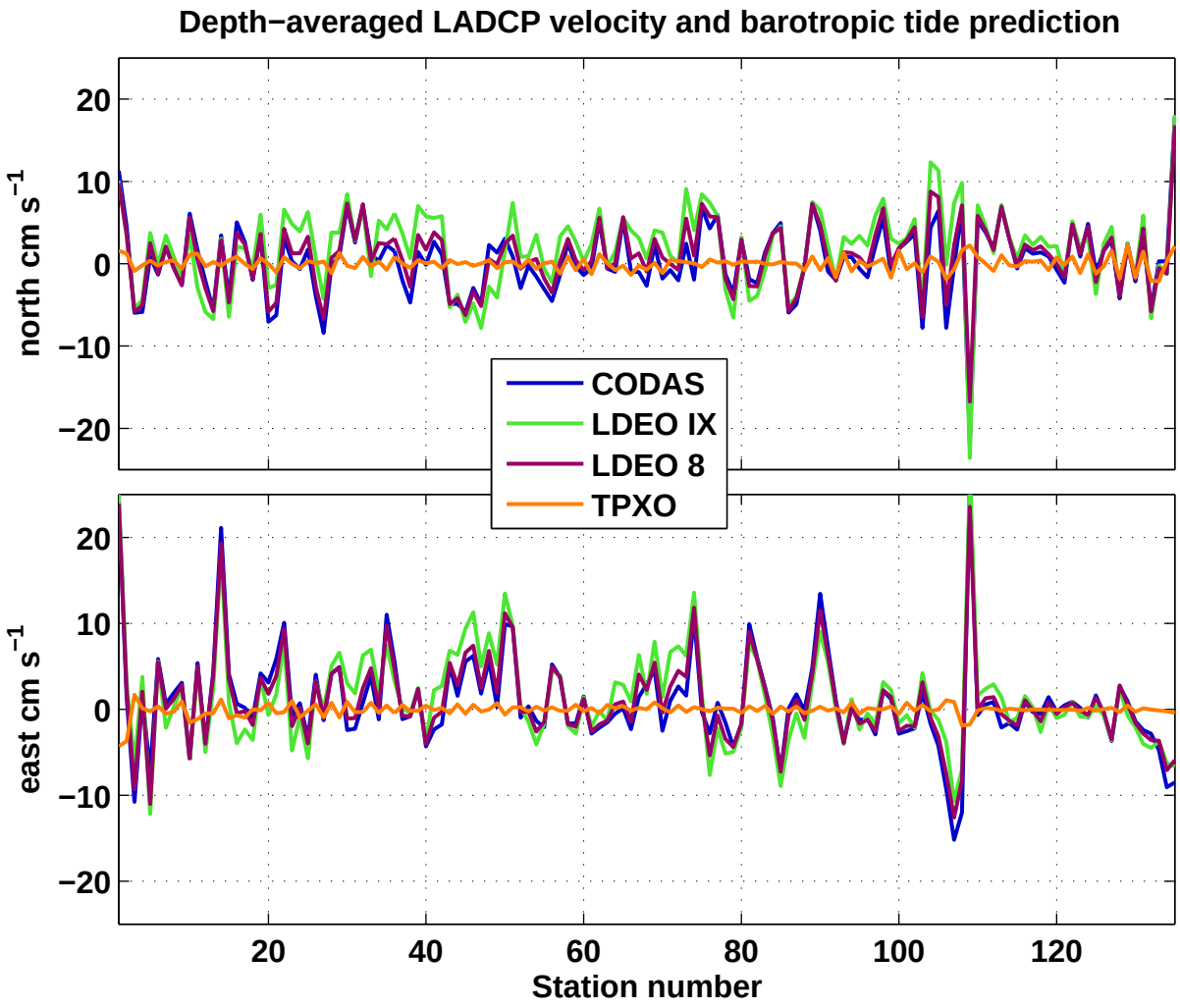

Figure 8: Comparison of the depth-averaged velocity and the barotropic tide predicted by TPXO6.2.

Table 4: Pairwise comparison of velocity solutions. For each cast, the root-mean-square velocity difference was computed for each (u,v) profile. The units are cm s^{-1}.

Cast	CODAS-IX		LDEO IX-8		CODAS-8	
	urms	vrms	urms	vrms	urms	vrms
001	0.94	2.32	1.49	2.11	1.03	2.24
002	3.14	3.06	1.86	1.35	2.50	3.05
003	5.97	1.68	4.25	1.66	2.32	1.93
004	3.13	3.24	1.98	1.66	2.03	2.29
005	6.54	3.57	2.23	2.48	4.92	2.71
006	2.75	1.92	0.84	1.65	2.47	1.08
007	5.55	2.01	3.54	2.02	3.23	1.57
008	3.43	2.81	2.00	2.72	3.07	1.97
009	4.33	6.03	2.18	1.62	2.47	5.03
010	1.79	3.92	1.03	3.39	1.50	2.74
011	2.21	6.85	2.47	5.25	2.97	2.72
012	4.04	6.04	2.78	4.46	2.45	2.98
013	2.90	3.53	2.20	2.01	1.33	1.87
014	6.11	3.58	5.17	3.05	5.29	2.14
015	4.53	4.20	4.68	3.13	2.96	2.55
016	7.71	5.07	5.95	2.26	2.66	3.54
017	4.60	2.12	3.97	1.51	2.43	1.92
018	5.19	4.03	2.95	3.55	2.59	3.35
019	3.29	4.06	2.04	3.65	2.14	2.04
020	6.89	5.07	4.09	3.91	3.07	3.09
021	6.22	5.36	3.58	2.76	3.74	3.37
022	3.45	4.48	3.00	3.08	1.60	2.78
023	6.57	6.17	4.25	5.83	3.73	2.09
024	3.36	5.69	2.64	3.52	1.40	3.12
025	4.06	6.20	4.18	4.30	2.62	4.25
026	3.47	6.67	3.67	6.72	2.66	4.22
027	2.28	6.17	1.56	4.01	1.83	3.30
028	1.88	6.26	1.68	4.62	1.81	3.98
029	3.71	4.40	2.93	4.19	2.76	3.85
030	6.93	3.22	6.09	4.14	2.94	3.15
031	6.64	3.80	4.12	1.56	3.88	3.71
032	8.44	3.66	5.52	1.63	3.62	3.00
033	5.78	3.10	3.27	2.51	2.90	1.72
034	3.79	7.72	2.75	5.84	1.84	4.03
035	5.82	4.81	5.50	8.40	5.11	6.73

Continued on next page

Table 4 – continued from previous page

Cast	CODAS-IX		LDEO IX-8		CODAS-8	
036	4.55	6.00	2.82	4.76	3.14	2.03
037	3.02	8.52	1.97	5.06	2.70	4.06
038	2.55	8.16	3.41	7.61	3.11	5.39
039	2.29	7.46	2.60	5.05	2.07	2.97
040	2.37	7.62	1.06	5.41	1.79	3.09
041	6.37	5.18	5.75	3.41	2.73	3.93
042	6.25	9.19	4.00	4.84	3.32	5.08
043	4.18	2.50	2.11	2.13	2.58	1.65
044	6.75	4.99	5.45	2.43	2.47	3.14
045	5.27	2.20	3.73	1.38	1.75	1.73
046	7.16	3.22	6.33	2.17	2.97	2.82
047	5.86	3.65	4.39	3.72	2.77	1.64
048	5.59	6.24	2.88	4.22	2.98	2.93
049	8.48	7.19	5.99	5.55	3.66	3.33
050	4.01	2.45	3.54	2.30	2.16	2.50
051	5.57	8.77	3.08	6.63	2.96	3.40
052	2.03	6.44	4.02	3.98	4.39	7.48
053	3.71	2.98	1.98	1.82	3.55	1.94
054	3.60	6.26	2.29	5.12	1.98	3.18
055	2.14	4.05	2.64	2.20	2.55	3.46
056	2.24	2.90	1.64	2.46	1.18	2.32
057	2.78	7.27	2.48	5.07	1.91	3.81
058	1.91	4.34	1.48	2.00	1.85	3.92
059	3.64	4.04	2.21	3.66	2.43	2.50
060	1.28	2.65	0.67	2.24	1.35	1.81
061	2.84	4.23	0.92	3.01	2.62	1.91
062	3.00	3.38	4.59	4.07	4.56	4.35
063	1.73	1.57	0.72	0.93	1.78	1.90
064	4.94	4.61	3.69	2.28	1.98	2.59
065	3.88	2.11	2.69	1.25	1.73	1.65
066	4.05	7.96	3.64	7.01	3.71	3.97
067	5.63	6.12	2.86	3.59	3.41	3.54
068	2.54	4.83	1.49	2.71	1.45	2.97
069	4.11	5.28	3.52	1.72	1.85	4.07
070	5.01	9.01	2.06	4.33	3.26	5.20
071	8.14	4.92	5.83	2.24	2.95	3.00
072	6.19	5.90	3.90	3.81	2.90	3.48
073	5.44	9.63	3.02	5.35	3.81	4.63
074	3.07	7.66	2.43	4.31	1.83	4.26

Continued on next page

Table 4 – continued from previous page

Cast	CODAS-IX		LDEO IX-8		CODAS-8	
075	2.99	2.10	1.69	1.71	1.87	1.69
076	7.68	3.77	3.99	2.68	3.87	1.98
077	4.72	1.23	2.34	1.24	3.59	0.99
078	5.98	3.39	2.64	2.81	3.85	1.70
079	1.84	4.12	1.28	3.30	1.93	1.92
080	1.95	0.98	1.07	1.57	2.16	1.54
081	3.35	3.91	2.21	3.18	1.55	4.49
082	1.91	2.26	1.58	1.73	1.77	1.47
083	2.29	3.58	2.16	2.56	1.71	1.98
084	3.13	1.45	3.01	1.52	1.14	1.08
085	2.57	1.45	2.60	1.77	2.82	1.85
086	6.49	4.06	5.00	2.88	4.14	4.01
087	4.00	3.14	3.62	3.46	2.70	4.12
088	4.47	1.40	3.17	1.94	2.41	1.44
089	4.05	2.43	2.29	2.98	2.75	4.38
090	7.96	4.47	4.09	3.37	5.13	3.51
091	3.15	4.10	1.67	3.11	2.06	2.78
092	3.37	1.86	2.06	1.77	2.24	1.63
093	2.67	4.57	1.74	3.17	2.45	1.89
094	1.87	3.44	2.65	7.19	3.52	8.12
095	3.18	5.79	2.74	3.76	3.59	4.07
096	1.98	6.25	1.39	3.82	1.68	3.96
097	3.39	6.48	1.84	2.94	3.44	5.10
098	1.64	4.64	1.25	2.90	1.33	4.66
099	2.51	9.69	2.02	5.33	1.54	6.48
100	2.31	2.45	1.32	1.22	2.33	2.04
101	2.64	1.98	2.09	1.27	1.90	1.40
102	2.64	3.87	0.90	1.64	2.03	2.69
103	3.05	4.31	1.52	2.08	2.67	2.39
104	2.57	11.54	1.66	4.78	2.37	6.86
105	4.06	6.81	3.69	5.66	2.65	3.32
106	6.29	12.14	4.97	7.23	3.47	5.55
107	5.17	13.26	2.70	8.45	3.55	5.16
108	5.02	10.20	2.35	7.26	3.24	4.09
109	2.15	5.42	8.63	12.54	2.47	9.99
110	3.13	4.07	2.51	2.70	2.65	3.31
111	3.81	3.32	2.75	2.47	2.20	3.33
112	3.49	3.01	2.37	1.19	2.46	2.43
113	5.16	2.42	2.87	1.54	2.78	2.02

Continued on next page

Table 4 – continued from previous page

Cast	CODAS-IX		LDEO IX-8		CODAS-8	
114	2.74	1.40	1.24	1.07	3.15	1.43
115	3.68	2.92	1.35	1.44	3.28	2.41
116	3.25	4.09	1.09	1.65	2.88	3.59
117	1.50	2.34	1.45	1.96	2.32	2.05
118	2.93	2.87	1.82	1.69	1.78	2.57
119	2.08	2.14	1.58	1.29	1.45	1.82
120	2.68	4.11	1.20	3.53	2.84	1.89
121	4.33	2.84	2.73	2.42	2.33	1.54
122	2.24	1.70	1.11	1.62	1.51	2.69
123	3.16	1.86	1.23	1.29	2.28	1.62
124	2.03	2.88	2.06	2.48	2.63	2.15
125	2.15	4.22	1.91	2.54	1.31	2.83
126	2.04	1.78	1.11	1.28	1.33	1.05
127	2.17	2.07	1.62	1.79	1.78	1.01
128	2.83	1.75	1.35	0.69	1.83	1.77
129	2.88	1.32	1.75	0.62	1.63	1.51
130	1.51	1.26	1.05	0.93	1.16	1.22
131	3.33	3.50	1.72	1.98	2.01	1.72
132	3.63	1.84	1.45	1.59	3.23	1.45
133	2.00	1.99	0.82	1.49	2.10	2.39
134	2.96	1.91	2.67	1.69	3.27	3.08
135	2.86	1.33	2.94	1.98	0.69	1.02